INORGANIC CHEMISTRY

FRONTIERS

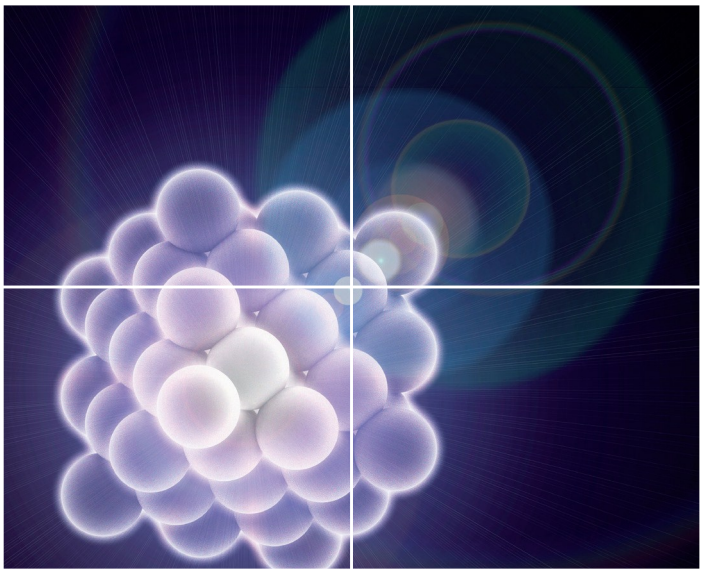

Accepted Manuscript

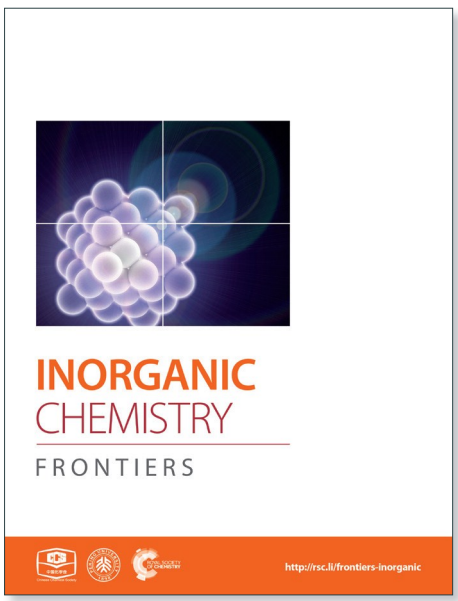

This is an *Accepted Manuscript*, which has been through the Royal Society of Chemistry peer review process and has been accepted for publication.

Accepted Manuscripts are published online shortly after acceptance, before technical editing, formatting and proof reading. Using this free service, authors can make their results available to the community, in citable form, before we publish the edited article. We will replace this *Accepted Manuscript* with the edited and formatted *Advance Article* as soon as it is available.

You can find more information about *Accepted Manuscripts* in the **Information for Authors**.

Please note that technical editing may introduce minor changes to the text and/or graphics, which may alter content. The journal's standard **Terms & Conditions** and the **Ethical guidelines** still apply. In no event shall the Royal Society of Chemistry be held responsible for any errors or omissions in this *Accepted Manuscript* or any consequences arising from the use of any information it contains.

Inorganic Chemistry Frontiers

RESEARCH ARTICLE

Designing Structurally Tunable and Functionally Versatile Synthetic Supercontainers

Feng-Rong Dai, [a,b] Yupu Qiao [b] and Zhenqiang Wang [b]*

Received 00th January 20xx,
Accepted 00th January 20xx

DOI: 10.1039/x0xx00000x

www.rsc.org/

We describe the design of a new family of molecular containers, namely, type IV metal-organic supercontainers (MOSCs), which are constructed from the assembly of container precursor *p-tert*-butylsulfonylcalix[4]arene, Co(II) or Ni(II) ion, and angular flexible dicarboxylate linkers. The combination of structural robustness and tunability of these cylindrically-shaped MOSCs makes them highly attractive supramolecular hosts. The type IV MOSCs exhibit a diverse range of supramolecular functions, including their selective binding with cationic guests and their tunable activity to modulate both stoichiometric and catalytic reactions, which are not readily accessible in the molecular precursors.

Introduction

Molecular containers that possess well-defined nanoscale space capable of accommodating one or more guest molecules have attracted tremendous interest in recent years[1-7] owing to their aesthetic appeal and their applications in a wide array of areas, such as stabilization of highly reactive species,[8, 9] transportation of small molecules,[10] gas storage and separation,[11-14] sensing,[15, 16] and supramolecular catalysis.[17-20] Within various types of molecular containers, metal-directed coordination containers are of particular interest thanks in large part to the reversible and yet relatively robust nature of metal-ligand interactions.[21, 22] Recently, we reported a new class of coordination containers, termed metal-organic supercontainers (MOSCs),[23-26] which were assembled from divalent metal ions, sulfonylcalix[4]arene-based container precursors,[27, 28] and rigid carboxylate ligands. Three prototypes of MOSCs, namely, *face*-directed octahedra (type I),[23] *edge*-directed octahedra (type II),[24, 26] and barrel-shaped boxes (type III),[25] were obtained by using trigonal, linear, and angular-planar carboxylate linkers, respectively. Related supercontainer structures based on thiacalix[4]arenes were also recently reported by the groups of Liao[29, 30] and Hong.[31] Compared to previously known coordination containers, MOSCs are distinguished by their unique multi-pore architecture, featuring both *endo* and *exo* cavities. The presence of multiple remote binding domains in a single synthetic host is expected to provide unprecedented opportunities for designing complex functions, such as binding cooperativity and binding regulation that are widely employed in biology.[32]

We noted that the three prototypes of MOSCs share a common design element, i.e., their formation is strictly dictated by the geometry of the carboxylate linkers and their structures are relatively rigid.[33] Specifically, the assembly of type I, II, and III MOSCs is largely predetermined by the carboxylate linker possessing a C_3 symmetry, a linear (i.e., 180°) geometry, and an angular-planar geometry subtending an angle of 120°, respectively. While such strict geometrical requirements permit precise construction of targeted supramolecular entities from molecular precursors, the resulting MOSCs are compositionally less flexible and limited in the scope of physical and chemical functionalities that can be accessed.

We contemplated that a design strategy that necessitates less demanding geometrical constraints would accommodate a wider range of chemical moieties and lead to structurally tunable and functionally versatile MOSCs. Herein, we describe the assembly of a new family of coordination containers, namely, type IV MOSCs, which are built from two tetranuclear units[34] - each containing four divalent metal ions, one sulfonylcalix[4]arene, and one μ_4-oxygen species - bridged by four structurally flexible dicarboxylate linkers (Scheme 1). We show that the high directionality of the tetranuclear units allows the construction of a family of cylinder-shaped MOSCs from a series of angular flexible dibenzoate ligands sustaining a methylene (-CH_2-; **L1**), methyleneamino (-CH_2-NH-; **L2**), or

Scheme 1. Assembly of Type IV Metal-Organic Supercontainers.

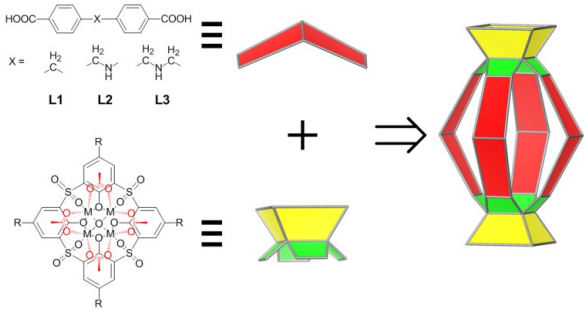

[a] State Key Laboratory of Structural Chemistry, Fujian Institute of Research on the Structure of Matter, Chinese Academy of Sciences Fuzhou, Fujian 350002, China
[b] Department of Chemistry, University of South Dakota
414 East Clark Street, Churchill-Haines Laboratories, Room 115
Vermillion, South Dakota 57069-2390, United States
Fax: (+1) 605-677-6397; E-mail: Zhenqiang.Wang@usd.edu.

Electronic Supplementary Information (ESI) available: Synthetic procedures, characterisation data, and spectroscopic titrations. See DOI: 10.1039/x0xx00000x.

bismethyleneamino (-CH_2-NH-CH_2-; **L3**) spacer, providing the desired, but otherwise elusive, structural flexibility and functional versatility. We demonstrate that these MOSCs preferentially bind with positively charged guests, which can be utilized to separate cationic dyes from anionic dyes. Most importantly, the type IV MOSCs exhibit supramolecular reactivity not accessible in the molecular precursors, including their capacity to stoichiometrically modulate the isomerization of Rhodamine B[35-37] and catalytically mediate Knoevenagel condensation.[38, 39] We further show that the capacity of the MOSCs to regulate chemical transformations can be judiciously tuned through manipulation of the carboxylate spacer, thus providing opportunities for designing novel catalytic reactivity.

Results and discussion

Synthesis and characterisation of type IV MOSCs

Three new MOSCs, namely, **1-Co**, **2-Co**, and **3-Ni**, were obtained as single-crystalline products from the reactions of Co(II) or Ni(II) and *p-tert*-butylsulfonylcalix[4]arene (TBSC) with three non-rigid dicarboxylate linkers, i.e., **L1**, **L2**, and **L3**, respectively. Structural analysis revealed that these type IV MOSCs share a cylindrical container topology which consists of two tetranuclear units bridged by four dicarboxylate linkers that adopt a V-shaped geometry (Figure 1). The tetranuclear units (Scheme 1), each possessing a μ_4-oxygen presumed to be from a neutral water molecule, closely resemble those in the previously reported MOSCs.[23-26] It is worth noting that although the linear length of the three dicarboxylate linkers increases in the order of **L1** < **L2** < **L3**, the longitudinal diameter of the cylindrical *endo* cavity of the resulting MOSCs shows a different trend in the solid state, following the order of **2-Co** < **1-Co** < **3-Ni**, with the O···O distance between the opposing μ_4-H_2O molecules reaching 7.28, 8.94 and 11.04 Å (excluding the sum of the atomic van der Waals radii), respectively. This is attributed to the structural flexibility of the dicarboxylate linkers, among which ligand **L2** assumes the most pronounced bending conformation. As a result, the lateral diameter of the *endo* cavity of **2-Co** becomes the widest among the three MOSCs (Figure 1). Owing to the non-symmetric nature of the -CH_2NH- spacer in **L2**, **2-Co** may in principle exist as several different isomers with its four N atoms arranged in either up or down configuration. This unfortunately cannot be determined by crystallographic analysis due to the high symmetry of the crystal structure. These interesting characteristics convey several important connotations that are of particular significance for designing functional versatility in MOSCs: 1) compared to other prototypes of MOSCs, the type IV congeners are indeed tolerant of a wider range of ligand conformations; 2) an array of chemical moieties are in principle compatible with and can thus be incorporated into type IV MOSCs; 3) the conformational freedom of the dicarboxylate linkers can potentially be utilized to regulate the molecular recognition capability of the MOSCs.

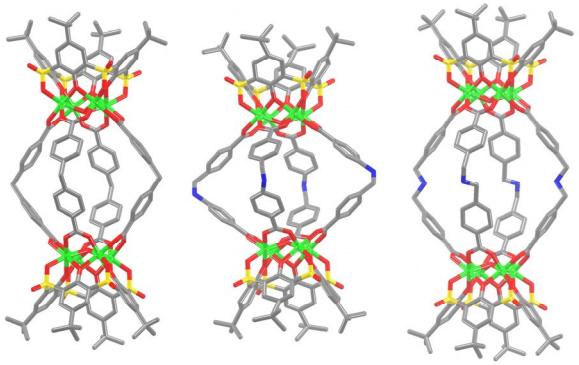

Figure 1. Structural representation of type IV MOSCs: (left) **1-Co** (X = -CH_2-), (middle) **2-Co** (X = -CH_2-NH-), and (right) **3-Ni** (X = -CH_2-NH-CH_2-). Color scheme: Co/Ni, green; S, yellow; O, red; C, gray; N, blue. Hydrogen atoms are deleted for clarity.

The trademark structural feature of MOSCs, i.e., the presence of both *endo* and *exo* cavities, is well retained in type IV MOSCs. Indeed, the X-ray crystal structure of **1-Co** clearly illustrates its capacity to utilize both binding domains for encapsulating guest species. In the as-synthesized **1-Co** crystal, a pair of *N*,*N*-dimethylformamide (DMF) molecules are trapped inside the *endo* cavity, while another pair of DMF molecules nestle inside the 'super' *exo* cavity formed through hydrophobic interactions among the *tert*-butyl groups of two TBSC units from adjacent MOSCs, resulting in an unusual one-dimensional (1D) tubular structure (Figure 2 and Figure S4). Four additional DMF molecules exist outside of the MOSC and **1-Co** can thus be formulated as {[Co_4(TBSC)(μ_4-H_2O)]$_2$(**L1**)$_4$(DMF)$_{2,endo}$(DMF)$_{2,exo}$}·4DMF. A similar tubular architecture is also observed in the crystal structure of **3-Ni** (Figure S5), although in this case, the guest species cannot be precisely located by X-ray crystallography due to the relatively poorer diffraction quality of the crystals. Interestingly, the solid-state packing of **2-Co** does not follow this same pattern, possibly due to its more bending conformation, which would have rendered the tubular packing less efficient; instead, it adopts the classic body-centered cubic packing (Figure S6).

To affirm the utility of type IV MOSCs as supramolecular hosts, their compositional purity and structural robustness were examined in a number of ways. Thermal gravimetric analysis (TGA) revealed that in a N_2 atmosphere, **1-Co**, **2-Co**, and **3-Ni** do not decompose until above 400 °C (Figure S7). Elemental analysis results suggested reasonable purity of the compounds (Table S2). Gas adsorption analysis indicated that the MOSCs show interesting solid-state porosity and exhibit

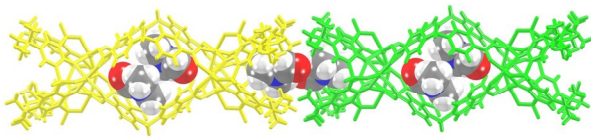

Figure 2. One-dimensional tubular assembly of **1-Co** with the encapsulation of DMF guest molecules in both *endo* and *exo* cavities. **1-Co** molecules (yellow and green) are represented in stick mode, while DMF molecules are represented in spacefilling mode.

intriguing O_2/N_2 and CO_2/N_2 selectivity (Figures S8-S13), similar to what was previously reported for type II MOSCs, which was attributed to a size-dependent packing collapse mechanism.[24] Mass spectrometry analysis suggested that the MOSCs, upon dissolution in chloroform (with a moderate to good solubility in the range of 10^{-6} M ~ 10^{-4} M), remain structurally intact (Figures S14-S16; Table S3). Together, these results confirmed the chemical purity and stability of these new MOSCs and the feasibility of probing their tunable functional properties in the solution phase.

Selective binding with cationic guests

We thus selected three organic dyes (Scheme 2), namely, methylene blue (MB), eosin Y (EY), and methyl orange (MO), as representative guests to probe the molecular recognition capability of type IV MOSCs. We first examined the host-guest chemistry at the liquid-liquid interface, as it has proven to be a useful platform for providing valuable guest-binding information.[24] Two immiscible solvents, i.e., water and chloroform, were chosen to afford the liquid-liquid interface due to the distinct solubility profiles of the hosts and the guests in these two solvents – while the dyes dissolve predominantly in an aqueous solution, the MOSCs are only soluble in chloroform. In the absence of MOSCs, chloroform extracted only a tiny fraction of MB and an even more negligible amount of EY or MO from the aqueous phase, as revealed by the ultraviolet-visible (UV-vis) spectra taken on the chloroform solutions after the extraction (Figure S17). However, when as little as 0.1 equivalent of a type IV MOSC, such as **1-Co**, was added to the chloroform solution, the water-soluble MB molecules were immediately coaxed into the organic phase upon shaking and mixing of the two layers (Figure S18). This stark contrast is attributed to, and a vivid indication of, the robust binding of **1-Co** with MB, which drives the partitioning equilibrium of the dye almost completely toward the chloroform phase, despite its otherwise insignificant chloroform solubility.

The favorable binding of **1-Co** with MB was further validated by UV-vis titration experiments,[40] which revealed a notable red-shift of the MOSC's absorption maxima (initially at ~ 348 nm) upon gradual increase of the MB equivalents in chloroform (Figure S19); fitting the titration data to the Benesi-Hildebrand (B-H) equation[41] gave rise to an apparent binding constant of $(2.18 \pm 0.20) \times 10^4$ (Figure S20), comparable to those found for type II MOSCs.[24] The MB/**1-Co** ratio at equilibrium in chloroform was estimated to be ~ 3 by comparing the MB concentrations (determined by UV-vis analysis) in the aqueous phase before and after the extraction (Table S4). This binding equivalent suggests that the MOSC is likely interacting with two molecules of MB through its two *exo* cavities (i.e., one MB per cavity) and another through its *endo* cavity. Interestingly, **1-Co** extracted neither EY nor MO in any substantial capacity under otherwise identical conditions, underlining an important bias against these two dyes (Figure S21). This can in principle be due to a size effect (i.e., EY, if not MO, is bulkier than MB), or a charge effect (i.e., EY and MO are anionic, whereas MB is cationic); we attribute the observed binding selectivity to the cationic nature of MB, since in control experiments, another cationic dye, Rhodamine B (*vide infra*), which is comparable in size to EY, can be efficiently extracted by **1-Co** (Figure S22). Similar binding selectivity favoring cationic guests was also apparent for **2-Co**, and to a lesser extent, **3-Ni**[42] (Figures S23-24). These results thus suggest that the electrostatic interactions between positively charged guests and electronegative oxygen atoms abundantly present in type IV MOSCs may play an important role in modulating their guest-binding affinity. A perhaps even more plausible factor contributing to the observed binding selectivity is the now widely-recognized 'cation-π' interaction,[43] which would involve the aromatic moieties of the MOSCs interacting with the positive charges of the dyes.

Separation of dye mixtures

Encouraged by the above intriguing findings, we decided to determine if the binding selectivity of type IV MOSCs can be utilized to separate cation-anion mixtures. Thus, two aqueous solutions containing a mixture of MB-EY (1:1) and MB-MO (1:1), respectively, were prepared. While the color of the individual dye solutions appeared as blue (MB), orange (EY), or yellow (MO), the two mixture solutions emerged in purple (MB-EY) or green (MB-MO) color (Figure S25). It was noteworthy that the chloroform solubility of the dyes in the form of cation-anion mixtures appeared to be enhanced even in the absence of any MOSC (Figure S26), presumably due to the formation of neutral

Scheme 2. Structures of three organic dyes used in this study.

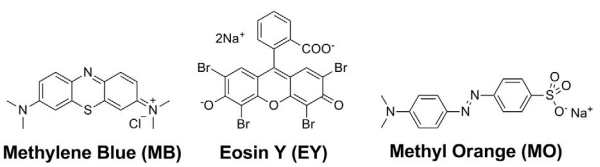

Methylene Blue (MB) Eosin Y (EY) Methyl Orange (MO)

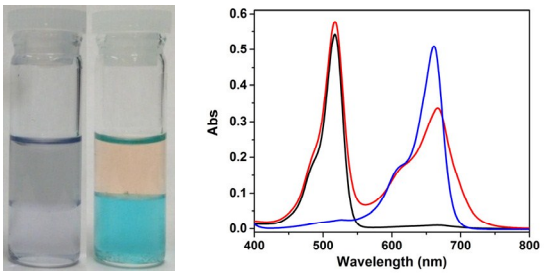

(*a*) (*b*)

Figure 3. (*a*) Liquid-liquid extraction of methylene blue (MB)-eosin Y (EY) mixture in the absence (left) and presence (right) of **1-Co**. Top layer: aqueous solution; bottom layer: $CHCl_3$ solution. The MB-EY mixture was initially dissolved in the aqueous solution and **1-Co** was dissolved in $CHCl_3$. (*b*) *red curve*: UV-vis spectrum of initial MB-EY mixture in aqueous solution; *black curve*: UV-vis spectrum of the aqueous phase after extraction by **1-Co**; *blue curve*: UV-vis spectrum of the $CHCl_3$ phase after extraction by **1-Co**.

ion-pairs that are inherently more soluble in low-polarity solvents such as chloroform.

The separation experiments were carried out at the liquid-liquid interface with the dye mixture initially dissolved in the aqueous phase and the MOSC in the chloroform phase. Taking the MB-EY mixture as an example, in the presence of **1-Co** (< 0.6 equiv.) and upon shaking and allowing the two layers to fully separate, the color of the aqueous phase changed from purple to orange, whereas the chloroform phase concurrently turned into blue (Figure 3a and Figure S27). These color changes clearly indicate the extraction of MB into the chloroform phase by **1-Co** and the retention of EY in the aqueous phase, giving rise to effective separation of the two dyes.

The separation was further validated by UV-vis measurements. Prior to the extraction, the aqueous solution of the dye mixture showed two major absorption bands centered at 517 nm and 665 nm, attributed to EY and MB, respectively (Figure 3b, red curve). Upon extraction, however, the absorption maximum at 665 nm disappeared from the aqueous phase (Figure 3b, black curve), whereas an intense absorption band centered at 661 nm appeared in the chloroform phase (Figure 3b, blue curve); meanwhile, the absorption maximum at 517 nm characteristic of EY in the aqueous solution remained largely unaltered (Figure 3b, black curve). This is in sharp contrast to the liquid-liquid extraction of the same MB-EY mixture in the absence of MOSC, where both MB and EY were partially extracted to the chloroform phase, presumably as an ion pair, as indicated by the appearance of two weak but well-defined absorption bands centered at 519 nm (EY) and 654 nm (MB), respectively (Figure S26). These UV-vis studies thus unambiguously confirmed that MB was fully extracted into the chloroform phase by **1-Co** and EY largely remained in the aqueous phase. Additionally, liquid-liquid separation was also successfully demonstrated for the MB-MO mixture using **1-Co** as the extractant (Figure S27); efficient separation of the mixtures was achieved in a similar manner when **2-Co** was used in place of **1-Co** (Figure S28). These results together point to the promising potentials of the type IV MOSCs for separation applications.

Stoichiometric modulation of Rhodamine B isomerization

In addition to exhibiting binding selectivity toward cationic guests, type IV MOSCs can also serve as 'molecular flasks'[44] for modulating chemical transformations. This was illustrated by their capacity to promote both stoichiometric and catalytic reactions, such as Rhodamine B isomerization and Knoevenagel condensation, respectively. During the course of examining Rhodamine B as a control guest as described above, it became apparent to us that the MOSCs were capable of mediating the otherwise well-documented intramolecular isomerization of the dye, which involves interconversion between the ring-opened, pink-colored cationic form (RB) and the ring-closed, colorless, neutral lactone form (known as Rhodamine B base, RBB) (Scheme 3).[35-37] The isomerization is known to be influenced by several experimental parameters, including the polarity and *p*H of the solvent that the dye dissolves in. Specifically, higher basicity or lower polarity favors the RBB form, whereas lower basicity or higher polarity promotes the RB form. In an aqueous solution (i.e., a polar environment), the dye shows an intense pink color and strong absorption in the visible range (~ 552 nm), characteristic of the cationic RB form. At the liquid-liquid (H_2O-$CHCl_3$) interface and in the absence of any MOSC, the RB form was found to remain in the aqueous phase, but only for a short amount of time (Figure S29). If the two layers were let sit for a longer period, the intense pink color of the aqueous phase eventually faded and a very light pink color became visible in the chloroform phase (Figure S30). We ascribe this to the effect of the weakly polar chloroform inducing a gradual conversion of the cationic RB form to the neutral, colorless RBB form. The latter is substantially more stable and soluble in chloroform than in aqueous solution, thus driving the partition equilibrium of the dye toward the organic phase. The light pink color of the chloroform phase is due to the small percentage of the RB form in equilibrium with the RBB form (Figure S30).

When **1-Co** was added to the chloroform phase, the color of the aqueous phase quickly faded but a rather intense pink color vividly appeared in chloroform (Figure S31), suggesting that the RB form was not only extracted into the chloroform phase (as described above), but it also remained predominantly as the colored, ring-opened, cationic form, despite the low polarity of chloroform which would have otherwise favored the colorless RBB form. This observation was further corroborated by UV-vis measurements taken on the chloroform phase after the extraction, which revealed a significantly increased intensity of the absorption maximum at ~ 547 nm, characteristic of the RB form, compared to that of the chloroform phase in the absence of any MOSC (Figure S32). A similar effect was also observed when **2-Co** or **3-Ni**[42] was present in the chloroform phase (Figure S32). These findings suggest that type IV MOSCs can indeed stabilize the RB form in solvents of low polarity (e.g., chloroform), most likely via encapsulating the dye molecule within their nanocavities.

To further interrogate the role that the MOSCs play in modulating the Rhodamine B isomerization, we carried out UV-vis titration experiments in homogeneous solution, where an increasing amount of **1-Co** was gradually added to a chloroform solution of the ring-closed RBB form. Upon the addition of **1-Co**, the UV-vis absorption due to the ring-opened RB form quickly grew in intensity, approaching saturation upon reaching a [MOSC]/[RBB] molar ratio of one (Figure 4 and Figure S33). Titrating the RBB solution with **2-Co** similarly led to the formation of the RB form, albeit with a lower efficiency (Figure 4 and Figure S34). Notably, when the container precursor TBSC was added as the titrant, no obvious isomerization beyond the

Scheme 3. Intramolecular isomerization of Rhodamine B dye.

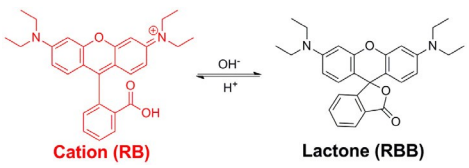

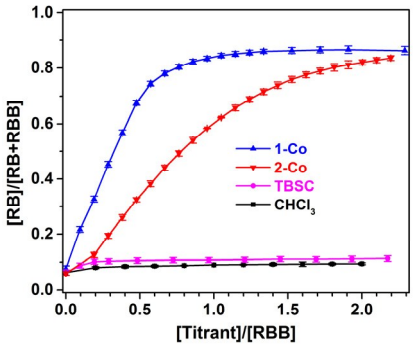

Figure 4. Fraction of the ring-opened RB form converted from the ring-closed RBB form as a function of the titrant equivalent when a chloroform solution of the RBB form was gradually titrated with **1-Co**, **2-Co**, TBSC, or chloroform. The results were based on the average of three independent trials for each titrant.

background reaction (i.e., when chloroform was titrated instead) was observed (Figure 4 and Figure S35). These findings strongly indicate that the modulation of Rhodamine B isomerization by type IV MOSCs mostly likely occurs inside the *endo* cavity. Furthermore, the MOSC-mediated conversion of RBB to RB in chloroform was found to be partially reversed by adding MB to the solution, as indicated by a decrease in the UV-vis absorbance attributed to the RB form (Figure S37). This can be explained on the basis that some of the RB cations were displaced by the competing, cationic MB molecules from the *endo* cavity, released into the bulk solvent, and subsequently converted back to the RBB form. In contrast, addition of MB to a TBSC-saturated Rhodamine B solution caused little change to the equilibrium (Figure S37). Extensive efforts have been devoted to grow single crystals of the host-guest complexes; unfortunately, weak diffraction quality of the crystals obtained has hampered an in-depth crystallographic analysis. We are currently investigating the exact mechanism of this interesting supramolecular reactivity in a number of ways, the findings of which will be communicated in due course, but several preliminary assessments can be made here: 1) we postulate that the active sites directly responsible for mediating the Rhodamine B isomerization involve the μ_4-H_2O located at the lower rim of the TBSC units and inside the *endo* cavity of the MOSC. Coordinating to four divalent metal ions makes the H_2O molecule a stronger Brønsted acid than usual and thus capable of releasing a proton to drive the formation of the RB form; 2) the chemical micro-environment of the binding cavity further furnishes the supramolecular reactivity. In this vein, the lower reactivity of **2-Co** may be due to its more distorted *endo* cavity and/or its methyleneamino moieties competing for the proton; 3) that the MOSC-mediated isomerization is stoichiometric is likely a result of the MOSC's stronger binding affinity (*vide supra*)[24] with the product (i.e., the cationic RB form) than with the substrate (i.e., the neutral RBB form), which translates to no catalytic turnover.

Catalytic mediation of Knoevenagel condensation

To gauge the MOSCs' capacity to facilitate truly catalytic reactions, we examined the classic Knoevenagel condensation, a well-known C-C bond forming transformation involving a nucleophilic addition of an active hydrogen-containing compound to a carbonyl substrate, often assisted by a Lewis-base catalyst.[38, 39] The ease with which the methylene group in **1-Co** can be modified into the methyleneamino moiety in **2-Co** or the bismethyleneamino moiety in **3-Ni,** without affecting the overall supercontainer architecture, makes type IV MOSCs particularly attractive as Lewis-base supramolecular catalysts.

To test their catalytic activity, a chloroform solution of 2-naphthaldehyde and malononitrile was treated with 1 mol% of **1-Co**, **2-Co**, and **3-Ni**, 4 mol% of **L3** methyl diester (**Me_2L3**), 2 mol% of TBSC, and no catalyst, respectively, at ambient condition for 48 h. The results revealed that TBSC and **1-Co** showed negligible reactivity for the reaction (Table 1), which was not unexpected, since they were not considered to contain any basic functionality. Surprisingly, despite the known Lewis basicity of its methyleneamino moieties, **2-Co** manifested only a very modest activity, achieving an unassuming 14% yield. In contrast, **3-Ni** was found to be a highly effective catalyst, promoting the Knoevenagel reaction nearly quantitatively (92% yield), presumably because of its stronger Lewis basicity in its bismethyleneamino groups, an aliphatic secondary amine. However, it is remarkable to note that an equivalent amount of **L3** methyl diester, which contains the same aliphatic secondary amine group, gave rise to a mere 19% yield, strongly indicating the importance of the 'cavity effect'. These findings thus highlight the exciting possibility of tuning the functional versatility of type IV MOSCs by virtue of their structural flexibility and robustness, and most importantly, the myriad of opportunities for designing novel supramolecular reactivity,[45, 46] an aspect we are currently actively pursuing in our laboratory.

Table 1. Yields of MOSC-catalyzed Knoevenagel condensation of 2-naphthaldehyde and malononitrile.[a]

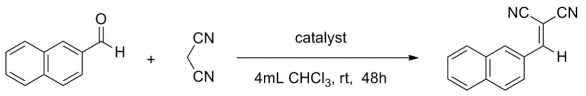

Catalyst:	None	TBSC	**Me_2L3**	**1-Co**	**2-Co**	**3-Ni**
Yield[b]:	2%	2%	19%	5%	14%	92%

[a] Reaction conditions: 2-naphthaldehyde (0.40 mmol), malononitrile (0.40 mmol), and catalyst (1 mol% of MOSC, 4 mol% of **Me_2L3**, or 2 mol% of TBSC) in $CHCl_3$ (4.0 mL) at room temperature for 48 h. [b] Isolated yields based on two independent trials.

Conclusions

In summary, we have demonstrated the design and synthesis of a new family of synthetic hosts, namely, type IV MOSCs, which are shown to be structurally tunable and functionally diverse.

The less stringent geometrical requirements of their design and the high chemical stability of their structure render these new supercontainers uniquely suited as 'nano-capsules' for modulating a wide range of molecular recognition events. The cavity-mediated binding selectivity and supramolecular reactivity of these MOSCs, which can be rationally tuned from bottom-up, provide hope for designing truly biomimetic functions, particularly in the context of molecular separation and supramolecular catalysis. We are currently addressing the exciting opportunities along these lines.

Acknowledgements

This work was supported by an NSF CAREER Award (CHE 1352279) and a South Dakota Board of Regents Competitive Research Grant. The authors also acknowledge an NSF MRI Award (CHE 1229035) for the purchase of a Bruker 400 MHz NMR spectrometer.

Notes and references

1. D. J. Cram and J. M. Cram, *Container Molecules and Their Guests*, The Royal Society of Chemistry, Cambridge, England, 1997.
2. N. Branda, R. Wyler and J. Rebek, *Science*, 1994, **263**, 1267-1268.
3. M. Fujita, D. Oguro, M. Miyazawa, H. Oka, K. Yamaguchi and K. Ogura, *Nature*, 1995, **378**, 469-471.
4. L. R. MacGillivray and J. L. Atwood, *Nature*, 1997, **389**, 469-472.
5. D. L. Caulder, R. E. Powers, T. N. Parac and K. N. Raymond, *Angew. Chem. Int. Ed.*, 1998, **37**, 1840-1843.
6. B. Olenyuk, J. A. Whiteford, A. Fechtenkötter and P. J. Stang, *Nature*, 1999, **398**, 796-799.
7. P. Ballester, M. Fujita and J. Rebek, Jr., *Chem. Soc. Rev.*, 2015, **44**, 392-393.
8. D. J. Cram, M. E. Tanner and R. Thomas, *Angew. Chem. Int. Ed. Engl.*, 1991, **30**, 1024-1027.
9. P. Mal, B. Breiner, K. Rissanen and J. R. Nitschke, *Science*, 2009, **324**, 1697-1699.
10. B. Therrien, *Top. Curr. Chem.*, 2012, **319**, 35-55.
11. J. An, R. P. Fiorella, S. J. Geib and N. L. Rosi, *J. Am. Chem. Soc.*, 2009, **131**, 8401-8403.
12. J. R. Li and H. C. Zhou, *Nat. Chem.*, 2010, **2**, 893-898.
13. T. Mitra, X. Wu, R. Clowes, J. T. A. Jones, K. E. Jelfs, D. J. Adams, A. Trewin, J. Bacsa, A. Steiner and A. I. Cooper, *Chem. Eur. J.*, 2011, **17**, 10235-10240.
14. A. Avellaneda, P. Valente, A. Burgun, J. D. Evans, A. W. Markwell-Heys, D. Rankine, D. J. Nielsen, M. R. Hill, C. J. Sumby and C. J. Doonan, *Angew. Chem. Int. Ed.*, 2013, **52**, 3746-3749.
15. R. Pinalli and E. Dalcanale, *Acc. Chem. Res.*, 2013, **46**, 399-411.
16. Y. Liu, X. A. Wu, C. He, Z. Y. Li and C. Y. Duan, *Dalton Trans.*, 2010, **39**, 7727-7732.
17. B. C. Pemberton, R. Raghunathan, S. Volla and J. Sivaguru, *Chem. Eur. J.*, 2012, **18**, 12178-12190.
18. M. D. Pluth, R. G. Bergman and K. N. Raymond, *Science*, 2007, **316**, 85-88.
19. M. Yoshizawa, M. Tamura and M. Fujita, *Science*, 2006, **312**, 251-254.
20. S. H. Leenders, R. Gramage-Doria, B. de Bruin and J. N. Reek, *Chem. Soc. Rev.*, 2015, **44**, 433-448.
21. P. J. Stang, *J. Am. Chem. Soc.*, 2012, **134**, 11829–11830.
22. T. R. Cook and P. J. Stang, *Chem. Rev.*, 2015, **115**, 7001-7045.
23. F.-R. Dai and Z. Wang, *J. Am. Chem. Soc.*, 2012, **134**, 8002-8005.
24. F.-R. Dai, U. Sambasivam, A. J. Hammerstrom and Z. Wang, *J. Am. Chem. Soc.*, 2014, **136**, 7480-7491.
25. F.-R. Dai, D. C. Becht and Z. Wang, *Chem. Commun.*, 2014, **50**, 5385-5387.
26. N. L. Netzer, F.-R. Dai, Z. Wang and C. Jiang, *Angew. Chem. Int. Ed.*, 2014, **53**, 10965-10969.
27. H. Kumagai, M. Hasegawa, S. Miyanari, Y. Sugawa, Y. Sato, T. Hori, S. Ueda, H. Kamiyama and S. Miyano, *Tetrahedron Lett.*, 1997, **38**, 3971-3972.
28. N. Morohashi, F. Narumi, N. Iki, T. Hattori and S. Miyano, *Chem. Rev.*, 2006, **106**, 5291-5316.
29. M. Liu, W. P. Liao, C. H. Hu, S. C. Du and H. J. Zhang, *Angew. Chem. Int. Ed.*, 2012, **51**, 1585-1588.
30. Y. Bi, S. Du and W. Liao, *Coord. Chem. Rev.*, 2014, **276**, 61-72.
31. K. Xiong, F. Jiang, Y. Gai, D. Yuan, L. Chen, M. Wu, K. Su and M. Hong, *Chem. Sci.*, 2012, **3**, 2321-2325.
32. B. Alberts, A. Johnson, J. Lewis, D. Morgan, M. Raff, K. Roberts and P. Walter, *Molecular Biology of the Cell*, Garland Science, 6th edn., 2015.
33. Q. F. Sun, J. Iwasa, D. Ogawa, Y. Ishido, S. Sato, T. Ozeki, Y. Sei, K. Yamaguchi and M. Fujita, *Science*, 2010, **328**, 1144-1147.
34. T. Kajiwara, T. Kobashi, R. Shinagawa, T. Ito, S. Takaishi, M. Yamashita and N. Iki, *Eur. J. Inorg. Chem.*, 2006, 1765-1770.
35. R. W. Ramette and E. B. Sandell, *J. Am. Chem. Soc.*, 1956, **78**, 4872-4878.
36. U. K. A. Klein and F. W. Hafner, *Chem. Phys. Lett.*, 1976, **43**, 141-145.
37. I. Rosenthal, P. Peretz and K. A. Muszkat, *J. Phys. Chem.*, 1979, **83**, 350-353.
38. E. Knoevenagel, *Ber. Dtsch. Chem. Ges.*, 1898, **31**, 2596-2619.
39. B. List, *Angew. Chem. Int. Ed.*, 2010, **49**, 1730-1734.
40. C. A. Schalley, *Analytical Methods in Supramolecular Chemistry*, Wiley, 2012.
41. H. A. Benesi and J. Hildebrand, *J. Am. Chem. Soc.*, 1949, **71**, 2703-2707.
42. The less pronounced effect observed for **3-Ni** is attributed to its lower solubility in chloroform than **1-Co** and **2-Co**.
43. D. A. Dougherty, *Acc. Chem. Res.*, 2013, **46**, 885-893.
44. M. Yoshizawa, J. K. Klosterman and M. Fujita, *Angew. Chem. Int. Ed.*, 2009, **48**, 3418-3438.
45. J. Lee, O. K. Farha, J. Roberts, K. A. Scheidt, S. T. Nguyen and J. T. Hupp, *Chem. Soc. Rev.*, 2009, **38**, 1450-1459.
46. M. Zhao, S. Ou and C. D. Wu, *Acc. Chem. Res.*, 2014, **47**, 1199-1207.

Table of Contents

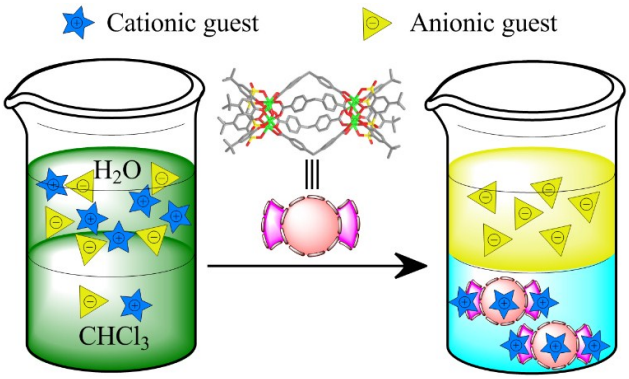

A new family of metal-organic supercontainers exhibit selective binding with cationic guests and tunable catalytic activity not accessible in molecular precursors.